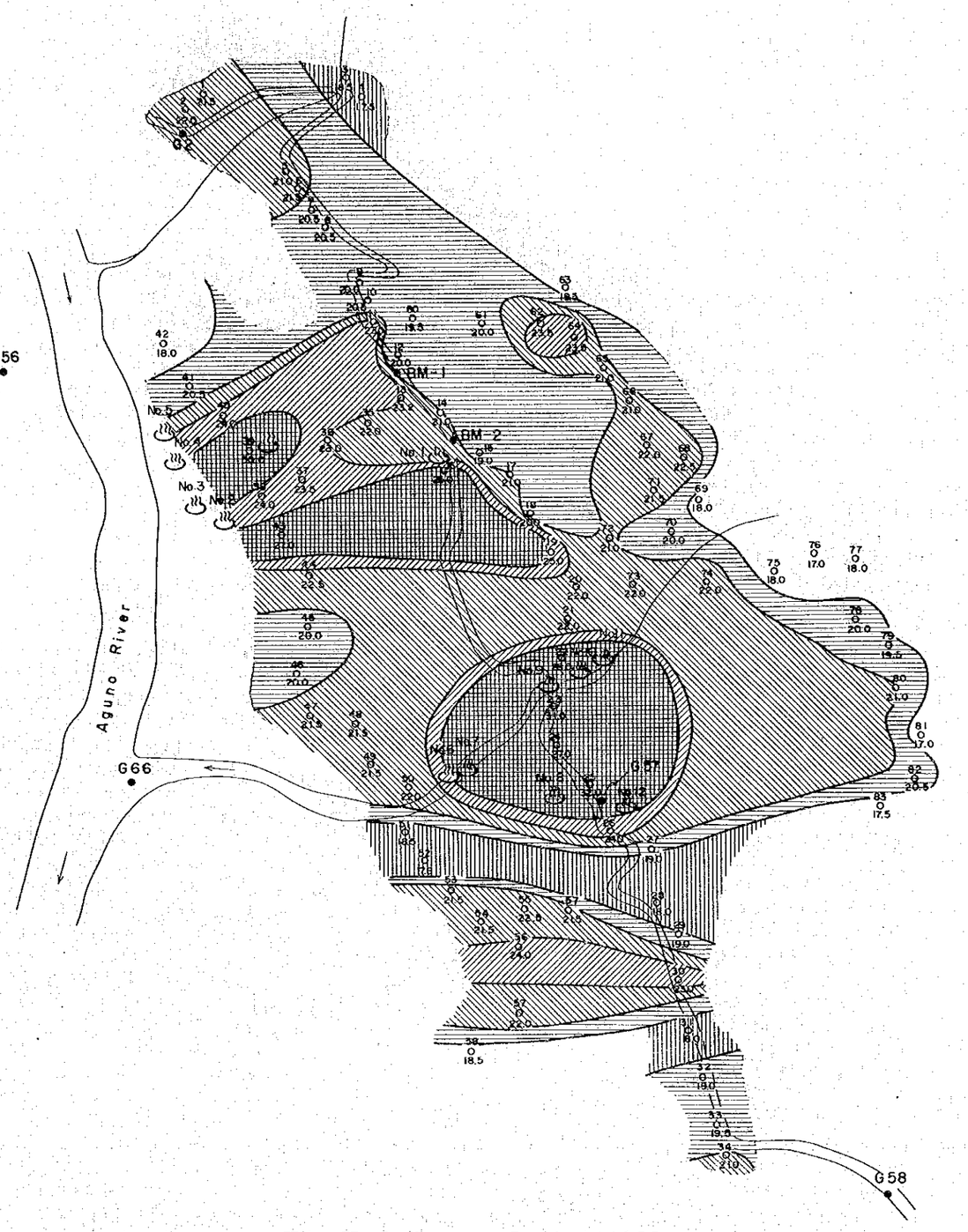

LEGEND

73	Hole No.	> 25.0℃
o	1m depth hole	
22.0	Measured temperature (℃)	23.0~24.9℃
G	Gravity observation point	
BM	Bench mark	21.0~22.9℃
	Hot spring	19.0~20.9℃
No.	Collected sample	< 18.9℃

Fig. II–2–5 Isothermal Map

Table II–2–2 Water and Gas Samples in Buguias

Sample	Temp. °C	pH	Remarks/Location
No 1	62.0	6.10	Hot water flow out from cracks trending N-S with moderate gas bubbling and flow. Extensive iron oxide coating of surrounding rocks. Located a few meters downstream from Man-atong bridge.
		*******	Gas sample taken for analysis.
No 2	56.0	6.60	Nearest to Man-atong creek terminal along Agno. River trending S-N. Surrounded with other thermal manifestation and vegetation common to hotsprings habitat.
			One water sample was taken solely for Manila laboratory.
No 3	55.0	6.20	Approximately 40 meters WN of No. 2 almost located along the bank of the river but of higher elevation. Thermal water flow out from recent elastics into the river in a horizontal travertine platform into the river.
No 4	58.0	6.40	Hot water flow out from the recent detrital deposit. Located along the bank of the river down north from Bug - 3.
No 5	55.0	6.20	Hot water flow out from travertine cementing the river clastics with moderate gas bubblings.
		*******	Gas sample taken for analysis.
No 6	60.0	6.20	Hot water flow out from travertine along the upper bank of mid-portion of Asinan Creek.
			Found above the big plunge of big boulders.
No 7	54.0	6.40	Hot water with moderate bubbling of CO_2 gas flow out on circular cracks of travertine on the opposite but lower bank and few meters upstream from Bug - 6.
		*******	Gas sample taken for analysis.
No 8	52.0	6.80	Not recommended for sampling. Located a few meters away from the bank of Kapangan Creek to the south.
No 9	71.0	6.35	High pressure spouting spouting flow out due to small opening in a travertine-domestic-like formation located at the junction of Sedel-Asinan Creeks located below the Asinan Bridge.
No 10	70.0	6.45	Hot water flow out from loose pebble formation near the Asinan bridge. Located a few meters away from the terminal of Sodel Creek.
		*******	Gas sample taken for analysis.
No 11	19.0	7.07	Lower Sodel Creek sample. Not recommended for sampling and analysis.
No 12	40.0	NA	Not recommended for sampling.
No 13	46.0	8.10	Taken in the western side of River Tutu-o around 100 meters elevation. Thermal water use for drinking purpose. Hot water flow out from unsolidified recent clastics.
No 14	17.0	6.60	Cold spring with intense iron oxide stainings at upper Sodel Creek. Located a few meters downstream of the Sodel water source.
No 15	20.0	8.0	Water taken from the upper Sodel upstream of No. 14.

KOH solution.

The chemical composition of water samples is shown in Table II–2–3 and the molecular ratio of the main component are also given in Fig. II–2–6.

Where fluide from the geothermal convection systems have reached the surface through springs or wells, the chemical and isotopic composition of these fields may indicate the subsurface temperature and flow patterns, as well as the recharge source, type of reservoir rock, and other important parameters of the system. Component concentrations or ratios that can be related to subsurface temperature are called geothermometers. According to Ellis and Fournier, quartz of neutral NaCl type hot water in geothermal reservoir is in equilibrium with the surrounding rocks, and therefore, the silica content in the discharge water may indicate the geothermal reservoir temperature. From temperature experiments of K-Feldspar and Na-Feldspar, the ratio of Na and K is suggestive of the underground temperature. Na, K, and Ca can be used for geothermometry as a tool for locating and evaluating prospective areas for geothermal development. The method employs the results of Tuesdell A.H. (1977) and Fournier R.O. et. al (1979) who found that molecular ratio data can be used to determine the last temperature at which water-rock equilibrium was attained. The calculation formulas used for geothermometry are as follows.

$$T_{SiO_2}\ (^\circ C) = (1315/5.205 \log SiO_2) - 273.15$$

where SiO_2 = mg/l

$$T_{Na-K}\ (^\circ C) = [\ 855.6/\log (Na/K) + 0.8573\ ] - 273.15$$

where Na, K = mg/l

$$T_{Na-K-Ca}\ (^\circ C) = \frac{1647}{\log (Na/K) + \frac{4}{3}\log (Ca/Na) + 2.24} - 273.15$$

where Na, K, Ca = mol/l

$$T_{Mg}\ (^\circ C) = T_{Na-K-Ca} - \Delta tMg$$

where $\Delta tMg = R = [\ Mg/(Mg + Ca + K)\ ] \times 100$

$$\Delta tMg\ (^\circ C) = 10.66 - 4.7415R + 325.87 (\log R)^2 - 1.032 \times 10^5 (\log R)^2/T - 1.968 \times 107 (\log R)^2/T^2 + 1.605 \times 10^7 (\log R)^3/T^2$$

where $T = T_{Na-K-Ca}\ (^\circ C)$

The Mg formula is available in case R is 5 – 50, and is not applied in case R is negative and $T_{Na-K-Ca}$ is below 70°C.

From the formulas stated above, the temperature of geothermal fluid in the reservoir was estimated as shown in Table II–2–4.

From the chemistry of the hot waters, the following evaluations are inferred:

1) All of the hot spring waters are of NaCl type (except for sample No. 13 at the west bank of the Agno river), indicating deep geothermal fluid.

2) Chemical characteristics of Sample No. 13 are different from the others in the area, containing poor Cl^- and rich SO_4^{--}. The temperature of hot water No. 13, however, is almost the same as the other springs. It therefore suggests a significant or major contamination of surface ground water associated with hydrogen sulfide (H_2S).

3) Ca and Mg contents are higher than that of the normal geothermal fluids in general and contains less Ca and Mg (Ellis, 1971). The hot spring water in the area therefore reasonably is considered that Ca and Mg were derived from the rocks into the hot water during the course of migration to the surface. In fact, the Buguias formation prevalent in the area consists of limestone and Mg rich basaltic pyroclastics.

4) The geothermometry computed by chemical components of the hot water shows that SiO_2 temperature is the lowest and Na-K-Ca temperature is the highest among calculated temperature.

5) SiO_2 geothermometry is generally applied in case the geothermal fluid comes out from the reservoir without any contamination with surface cold water. In this case, the hot spring water is diluted by cold water near the surface, even though the temperature is about 150°C.

It is therefore inferred that the actual temperature of the geothermal reservoir in the area would be higher than the calculated temperature.

6) Na-K and also Na-K-Ca of thermometers are calculated. However, Ca content of the fluid in the area is higher than the normal geothermal fluid as stated above. Therefore Na-K-Ca geothermometer is more reliable and it gives a temperature of about 250°C.

7) Mg content in the hot water is also high. Mg correction was made and it shows a temperature of about 190°C.

8) Temperature estimation based on the chemical composition fluctuates from 160° of silica to 250°C of Na-K-Ca, because the hot water is probably contaminated with surface cold water. Although the calculated temperature does not represent actual reservoir temperature in this field, it is possibly considered that the temperature in depth would be over 200°C from the computation of the chemical compositions.

Table II–2–3 Chemical Composition of Hot Springs and River Water

Chemical Component / Sample No.	Temp. °C	PH	CON μ℧/cm	TSM	Li^+	B^+	Na^+	K^+	Ca^+	Mg^+	Total Fe	Al^+	F^-	HCO_3^-	Cl^-	SO_4^{2-}	As	SiO_2	*SiO_2
Bug- 1	62	6.20	12200	7850	7.4	45	2270	315	321	38.6	2.96	0.05	0.12	715	3902	205.8	0.853	123.0	125.4
3	55	6.36	14100	9490	8.3	48	2680	378	418	35.2	3.59	0.06	0.19	848	4583	215.5	1.130	130.5	129.2
4	58	6.42	12800	8380	7.6	48	2350	332	360	36.2	2.44	0.08	0.14	784	4055	198.6	1.049	125.0	125.5
5	55	6.44	13550	9020	7.8	51	2580	345	366	36.2	3.04	0.06	0.22	867	4238	230.9	0.978	130.0	132.2
6	60	6.32	14100	9540	8.1	53	2590	358	404	37.2	8.65	0.10	0.16	2318	4431	230.9	1.969	123.5	121.7
9	71	6.52	16600	11190	9.7	61	3150	422	404	56.0	3.29	0.06	0.18	811	5315	243.5	1.146	142.0	142.0
10	70	6.60	14500	9620	8.5	52	2650	380	358	44.4	2.84	0.09	0.15	741	4563	217.9	0.944	132.5	129.8
13	46	7.42	782	585	<0.1	<1	108	4.4	60.8	3.1	0.10	0.02	0.25	68.6	16.26	293.1	0.020	38.0	44.3
14	17	6.70	897	655	<0.1	<1	15.5	1.6	102.5	21.9	1.28	0.03	0.05	642	2.64	3.3	0.000	39.0	46.4
15	20	7.32	180	125	<0.1	<1	7.0	0.8	24.9	6.3	0.09	0.01	0.02	104.1	3.25	7.4	0.000	22.5	29.9

*SiO_2 : colorimetric analysis

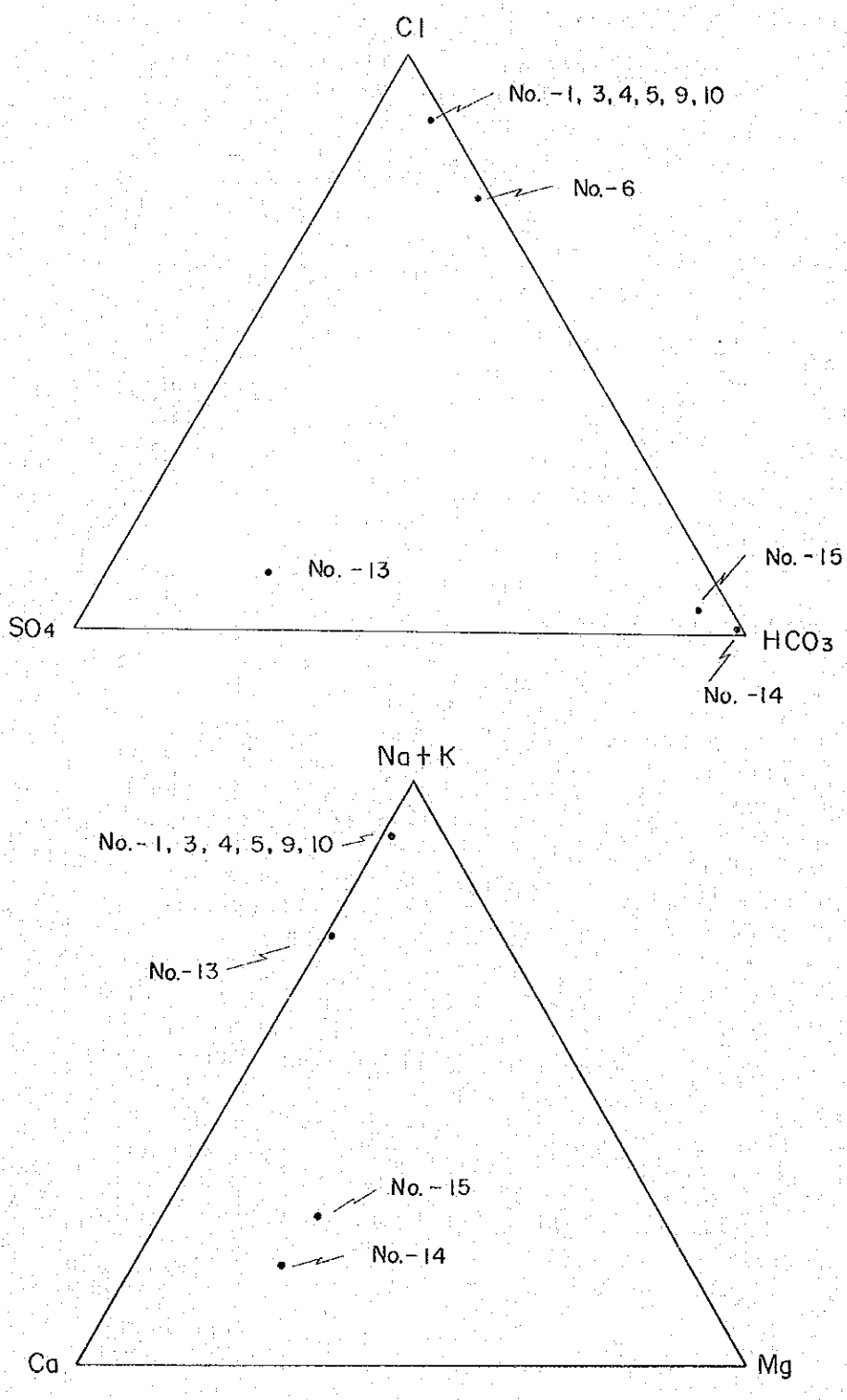

Fig. II–2–6 Diagram of Anion and Cation

Table II–2–4 Computed Chemical Geothermometry

Sample No.	T SiO_2 (°C)	T Na-K (°C)	T Na-K-Ca (°C)	T Na-K-Ca-Mg (°C)
Bug - 1	149	226	250	180
3	153	228	252	197
4	150	228	251	189
5	153	221	249	191
6	149	225	250	192
9	158	221	255	175
10	153	230	255	183

9) The distribution of geothermal manifestations in the area is limited in Buguias Central and chemical composition of the hot water shows the same characteristics as a whole.

In general, it is difficult to infer the location and the depth of high temperature reservoir from the result of geochemical exploration. However, some suggestions in this case regarding heat source in the area would be available from the data of Daklan area, which is located about 20 Km south of the area, and which was preceeded by a geothermal exploration. That is, the Quaternary dacite dome, which is presumed to be the heat source and rose at the same geological time as that of Daklan is distributed at the eastern end of the survey area.

CHAPTER 3 GRAVITY SURVEY

Chapter 3

Gravity Survey

3–1 Purpose of Survey

Gravity surveys are frequently utilized in the fields of oil, metal and geothermal exploration to analyze the subsurface structures from the differences of rocks and geologic formations. Based on rock densities, it is possible to analyze the basement structure, faults, graben, horst and latent intrusive rocks. Furthermore, gravity surveys are used to confirm the structures interpreted by geological surveys and other means of geophysical exploration.

In general, an isogravity map suggests the regional tectonic movement which controls the geological structures in a survey area. For this reason, gravity surveys are conducted during the initial stage of geothermal exploration. In fact, according to the gravity survey data gathered, most of the hot springs in Japan are located at or adjacent to large scale gravity lows. Among the operating geothermal power plants in Japan, OHNUMA, KAKKONDA, ONIKOBE, OHTAKE and HACHOOBARU were proven to be related to large scale gravity lows. Such large scale low anomalies suggest the presence of grabens and depressions at depths and are very effective in furnishing information about geothermal conditions.

3–2 Method of Survey

3–2–1 Abstract

The earth's gravity is a composite force combining the attraction due to the earth's mass and the centrifugal force caused by the earth's rotation. If the earth were a perfect sphere and its density distribution was spherically symmetrical, the gravity value would be the same anywhere on its surface.

Centrifugal force is maximum on the equator and zero on both poles, direction of action is always opposite that of gravity.

Therefore, gravity becomes maximum on the poles and minimum on the equator. The difference between the maximum and the minimum gravity values is 0.3% which is almost negligible.

A body on the surface of the earth has a "weight" which results from the gravitational attraction between the body and the entire earth. If the body is allowed to fall, it is accelerated by this weight. The unit of acceleration is the gal, named after Galileo and 1 gal is

1 cm/sec^2. The average acceleration on the earth's surface is about 980 cm/sec^2 = 980 gals (increases by about 0.3% from equator to pole).

Gravitational anomalies are only very small fractions of the earth's field, so a smaller unit is needed. The unit commonly used in gravity survey is the milligal or mgal which is 0.001 gal. Anomalies from local geologic structures are commonly in the order of one to ten mgals.

3–2–2 Survey Planning

Observation stations are shown on the Location map (Fig. II–3–1) made by the JICA survey team. Planned stations are 240 points and actual observation stations are 241. Among these, the altitudes of 132 points were measured by leveling, 8 points by traverse survey and the remaining 101 points were measured by a microbarometer.

The number of the stations are 1 to 241 consecutively, except gravity standard station No. 900. The survey area is about 140 Km^2, and the standard station interval is 500 m.

Although the observation stations were densely distributed around Buguias Central, the rest were set along mountain ridges and rivers because of rough topography in the area. Therefore, the stations could not be located with uniform density. Each location of the points was connected by transit or a pocket compass in order to increase accuracy.

3–2–3 Gravimeter

La Coste G. type gravimeter was used. Specification and functions are listed below.

Name of Instrument	La Coste G. type
No. of Production	G-236
Operating Range (mgal)	0.0 – 7440.760
Temperature of heater (°C)	47.5
Reading line	2.60
Date of production	July 1970
Dimensions (cm)	14 x 15 x 20
Meter weight (Kg)	8.6
Made by	La Coste Romberg (U.S.A.)

La Coste gravimeter is characterized by their worldwide range without the need of resetting, and the negligible drift is normally less than 0.5 mgal/month. Gravity values measured by this instrument ranges from 3,000 mgal to 4,000 mgal, whenever the station. is located in the middle latitude like in Japan, irrespective of the height of the station. In the low latitude countries like the Philippines, however, gravity values varies from 1,800

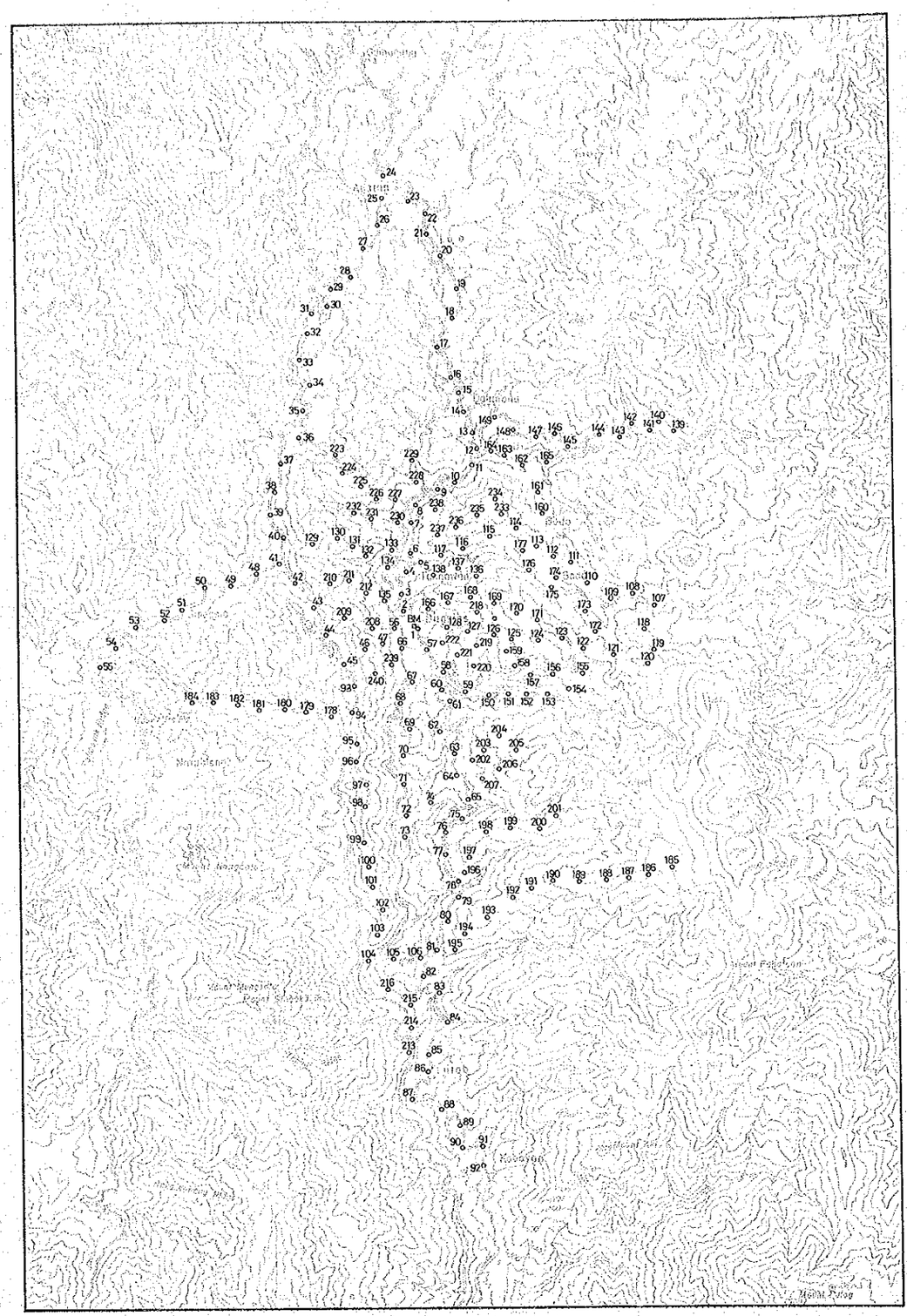

Buguias Geothermal Development Survey
the Republic of the Philippines

LOCATION OF GRAVITY OBSERVATION POINTS

0 1000 6000 km

Jan~Feb, 1981

Fig. II-3-1

mgal to 2,100 mgal.

The unique features of the La Coste gravimeter make it possible to measure gravity values in the Philippines without resetting the instrument and without drift corrections applied.

Each La Coste gravimeter has its own particular correction parameter. The range of correction values is variable with the elevation and latitude of the survey area. In this case the following correction value was adopted.

Table II–3–1 Milligal Value for LaCoste & Romberg, Inc. Model G Gravity Meter #236

Counter Reading	Value in Milligals	Factor for Interval
1,600	1,701.202	1.06352
1,700	1,807.554	1.06357
1,800	1,913.911	1.06360
1,900	2,020.271	1.06367

3–2–4 Comparison of Standard Gravity

In Northern Luzon Island, no IGSN (International Gravity Standardized Net) station has been established, in which case the survey was planned to determine the IGSN gravity value to be correlated with the known gravity point in Japan.

Thereafter, information of an international gravity standard point located at Muntinglupa Metro Manila was used as a gravity basepoint. Then, standard values in Japan were used for gravity comparison. The results of the comparison are shown on Table II–3–2 and the gravity standard set at Buguias camp N900 is calculated from those data. The standard value of this survey was set with comparison of value at N900 and Muntinglupa. However, the value was bigger by 19 mgal than the calculated one based on the value of the standard point in Japan. This is because the value of Muntinglupa belongs to the Potsdam system.

Principally, standard values should be adopted first, the value based on IGSN 71, but considering the connection with the gravity network in the Philippines, which is based on the standard point, g = 978,216.025 mgal was used for all gravity data in this case.

13159C is the gravity standard point set by Japan Geographical Institute, Meguro-Ku,

Tokyo and where BM6642 of the first order level point located at Kinugawa Hotspring, Shioya-gun, Tochigi Pref.

The drift value is only 0.233 mgal for 123 days so that the average drift rate becomes 0.0027 mgal/day and the gravity difference between Buguias N900 and BM6642 is about 1,600 mgal.

Table II–3–2 Gravity Standard Values

	13159C Tokyo	Muntinglupa	Buguias 900	BM 6642
Latitude	N 35° 38.6′	N 14° 22.5′	N 16° 43.4′	N 36° 50.6′
Longitude	E 139° 41.3′	E 121° 0.9′	E 120° 49.5′	E 139° 43.9′
Date of Observation	1981. 1. 16	1981. 1. 23	1981. 1. 30	1981. 5. 19
Time of Observation	14 h 39 m	18 h 6 m	8 h 2 m	9 h 12 m
Reading Value	3349.406	2020.060	1878.652	3421.386
Instrument Height (m)	0.21	0.27	0.23	0.26
Milligal Value	3562.851	2147.976	1997.565	3639.484
Earth Tide Correction (mgal)	− .073	− .035	− .0007	.072
Instrument Correction (mgal)	0.065	0.083	0.071	0.080
Corrected Value (mgal)	3562.843	2148.024	1997.629	3639.636
Drift Correction (mgal)	0.000	− 0.019	− 0.037	− 0.233
Corrected Value (mgal)	3562.843	2148.005	1997.692	3639.403
Gravity Difference (mgal)	0.000	(976218.464) 1414.838	(976218.465)	76.560
Gravity Value (mgal)	979763.190	978366.470	978216.057	979839.750

3–2–5 Leveling

The direct leveling method was adopted for 122 of 241 points by Auto level B-2 of Sokkisha, Japan. Basement of leveling is a triangular point with coordinate and elevation as follows.

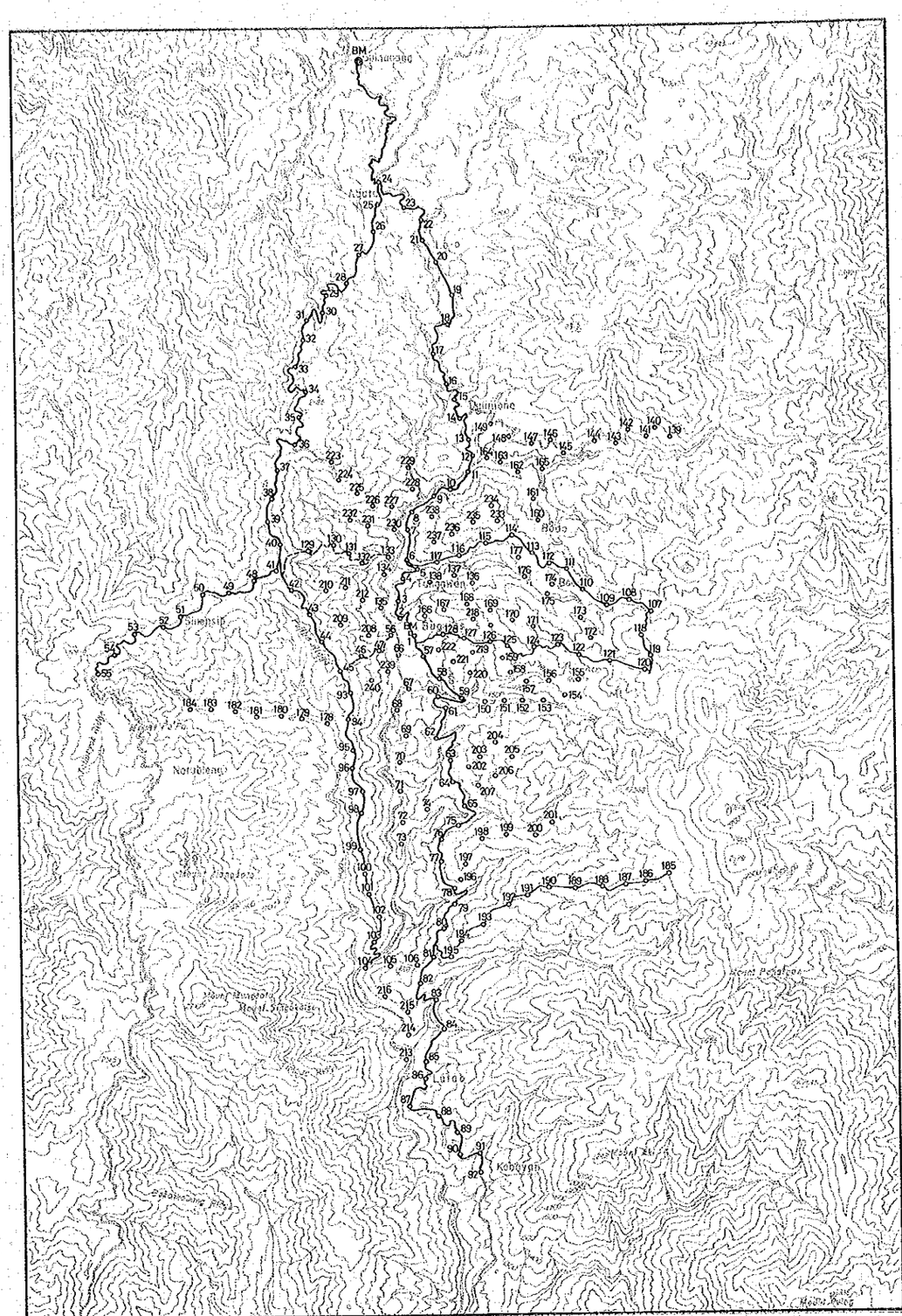

Bugulas Geothermal Development Survey
the Republic of the Philippines

ROUTE MAP OF LEVELLING SURVEY

0 1000 6000 km

Jan~Feb, 1981

Fig. II-3-2

Latitude N16°49′30″77

Longitude E120°49′0″04

Altitude 1503.55 m

In the leveling network, main roads were used for the leveling route, and the loop survey method was considered in order to minimize the accumulated error.

Traverse survey by GT60 of Sokkisha, Japan, in the course of loop survey was also conducted at 8 points, where the topography is very rough.

3–2–6 Survey by Microbarometric Altimeter

Altitudes of 101 points were measured by microbarometers made by American Paulin, U.S.A., excluding the points measured by leveling method and traverse survey. Two field altimeters (model MDM-5) were used, one as a moving barometer and the other as a stationary Base Barograph for the base point measurements.

On each reading corrections for temperature, pressure and closed error were made.

(1) Temperature correction

Air column correction values are determined by the following formula

$$\delta H = 0.00204 \cdot \Delta H (F - 50.0)$$

where, δH : Temperature correction value of two diffrent points

ΔH : Altitude difference of two different points

F : Average temperature of two different points (^{O}F)

The American Paulin System Altimeter is calibrated to measure directly the density of the air at 50°F. A temperature above or below this value will involve a change in density of the column of air being measured.

(2) Barometric Correction

In most cases, after a traverse has been made and the altimeter correction has been applied, temperature and elevation corrections with the true elevation at the base station should be noted. In this survey, a base barograph was used for the barometric correction.

(3) Closure error correction

As in leveling, a traverse starts from a point of known elevation and closed on the same point. The error of the traverse is time alloted on each reading after making the above-mentioned corrections.

3–3 Gravity Correction

Several corrections should be made on the observed gravity value to determine the real Bouguer anomaly.

3–3–1 Flow of Correction

The process of calculating the gravity value is shown by the following following diagram.

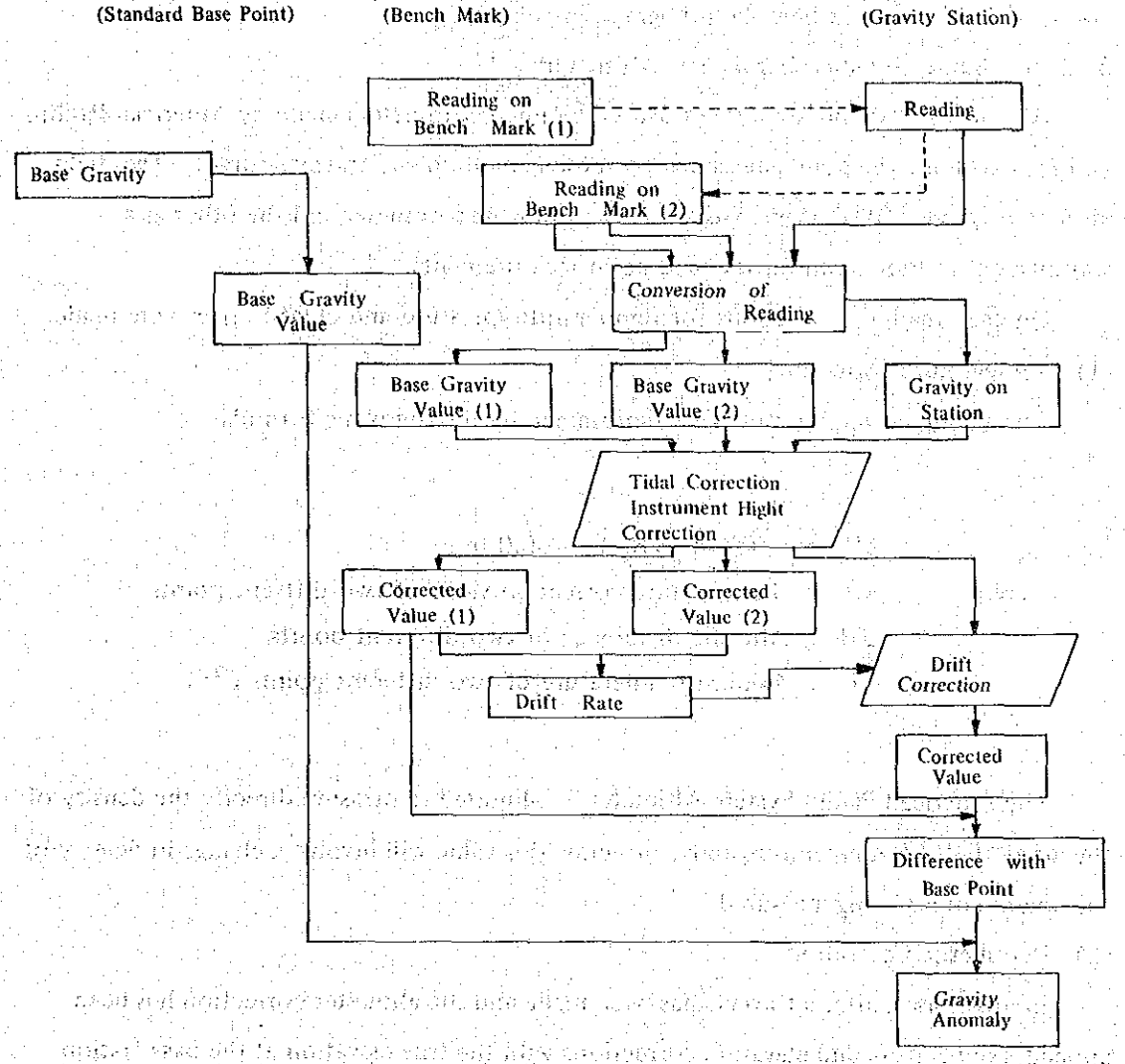

(1) Conversion

To obtain gravity in milligals from the reading of the counter and dial, a table of conversion is employed. In the table, the value of gravity in milligals is given for each 100 units of the counter. By using this table, and corresponding factor, the value of gravity for any reading indicated by the counter may be obtained.

$$Vrk = K + k\,(Vr - Vro)$$

Vrk : Observed gravity value

Vr : Reading indicated by the counter

Vro : Reading for each 100 units of the counter

K : Gravimeter Constant

k : Conversion factor

(2) Tidal correction

Tidal forces are due to the attraction of the sun and the moon at the earth's surface which deviates in direction, and intensity, with time and from place of observation.

Tidal force due to the sun and the moon is calculated by the following formula.

$$Vet = -\Sigma\ 1.16u$$

$$u = -\frac{3}{2} \cdot G \cdot M \cdot \frac{a}{r^3} \{3(\sin^2\delta - \frac{1}{3}) \cdot (\sin^2\varphi - \frac{1}{3}) + \sin 2\delta \cdot \sin 2\varphi \cdot \cos\theta + \cos^2\delta \cdot \cos^2\varphi \cdot \cos 2\theta\}$$

where,

Vet : Tidal correction

u : Tidal force of the planet

G : Gravitational constant

M : Mass of the planets (the sun and the moon etc.)

a : Distance from center of earth to observation point

r : Distance between earth and planet

δ : Declination of the planet (angle from equator to south or north)

φ : Latitude at observation point

θ : Angle of the planet (angle between terrestrial and planetary meridian plane)

In order to check the tidal corrections, gravity observations on a constant station have been made. Gravity values on the constant station changes together with the changes in tidal forces. The tidal force variations can be confirmed by observing changes for more than 12 hours.

Two peaks and bottoms were observed for 24 hours from 6:00 a.m. 5, Mar. to 6:00 a.m., 6 Mar. 1981 at N900 in Buguias.

Good agreement between values was observed with a slight scattering of +0.102 mgal on the peak and −0.197 mgal on the bottom. The error is only less than ten or more mgals.

(3) Instrument height correction

This correction is used to adjust the instrument height from the station elevation

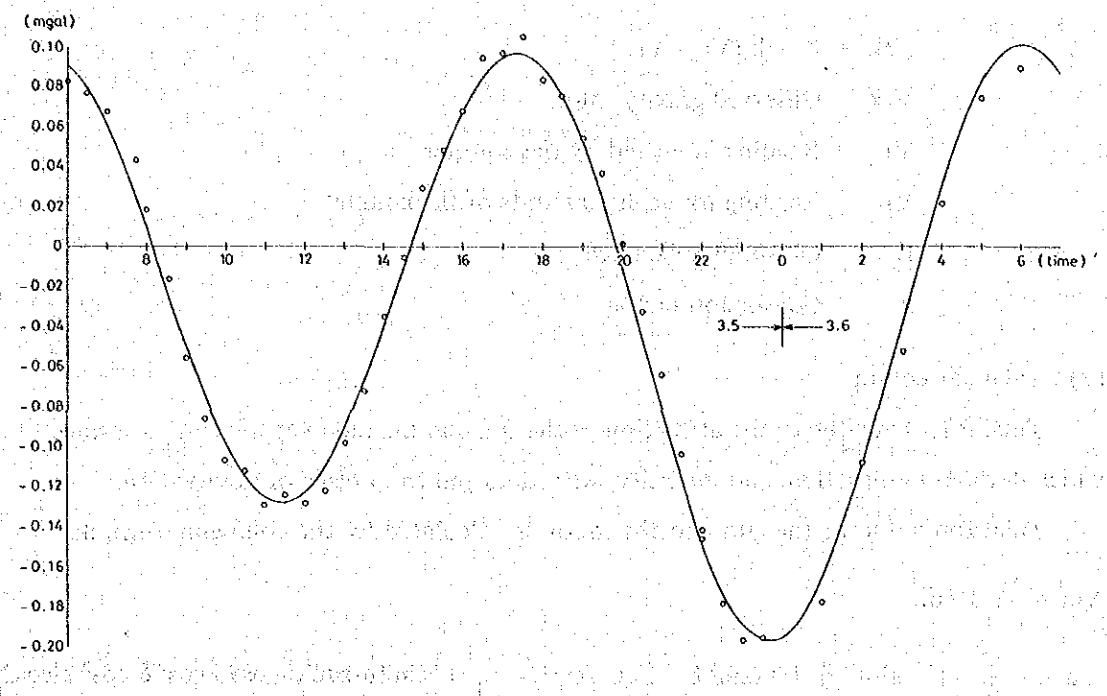

Fig. II–3–3 Diurnal Variation at Gravity Station

surveyed by leveling.

$$Vhi = 0.3086 \cdot hi \times 10^2$$

where,

Vhi : Correction of instrument height

hi : *Height from station level to top of gravimeter (cm)*

(4) Drift correction

Drift is an inherent characteristic error of a gravimeter which changes proportionally with time. The rate of change in drift is not always constant as it depends upon the characteristics of a gravimeter, temperature and pressure of the atmosphere and the way of handling of the instrument. So, in this survey the closure error was regarded as drift and distributed by time allotment.

(5) Gravity value

Corrections on the observed value are as follows:

$$Vc = Vrk + Vhi + Vd$$

where,

Vc : Corrected gravity value

Vrk : Observed gravity value

Vd : Drift correction value

The gravity value (g) is observed by adding a difference (Dg) of corrected gravity (Vc) and the corrected gravity at the bench mark (Vg) with a base point gravity (Bg), which has the same value as the international standard gravity.

$$Dg = Vc - Vg$$

$$g = Bg + Dg$$

3–3–2 Correction of Gravity

A flow chart of various corrections from a reading to a Bouguer anomaly is shown below.

(1) Free Air Correction

This is a required correction for the elevation of a gravity station because the measurement was made at a different distance from the center of the earth. The first term of the elevation correction is 0.3086 mgal/m. This is called the elevation correction together with Bouguer correction.

$$\delta g_O = 0.3086 \cdot Hm$$

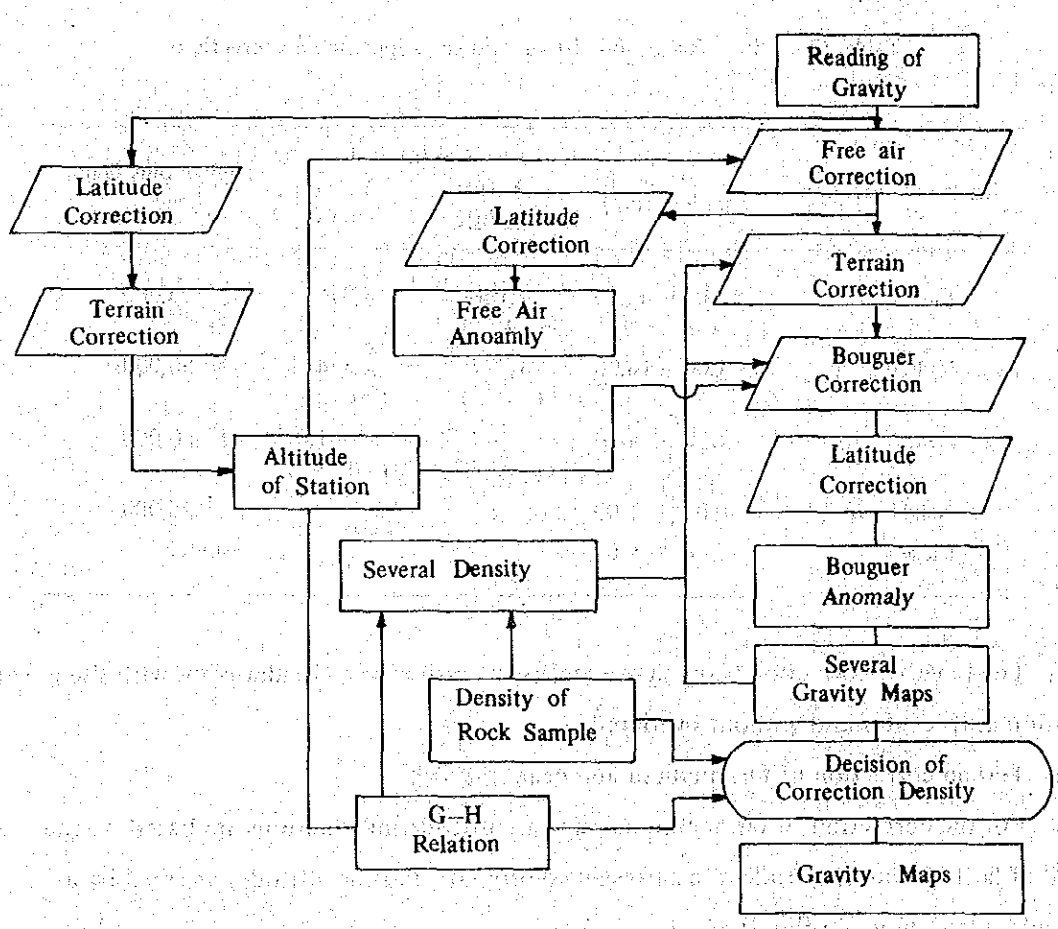

where,

δgo : Free air correction

Hm : Altitude of the station (m)

(2) Terrain Correction

A topographic irregularity (hill, knoll, slope, etc.) will exert an attraction directly proportional to its desntiy. The vertical component of this attraction will be directed upwards and this reduces the gravity.

A term of this magnitude must therefore be added to the measured value of gravity. A station near a valley is a negative mass and the vertical component of its attraction will also be directed upwards leading again to an additive topographic correction.

The topographic correction is calculated by dividing the area around a station in compartments into 5 groups, namely, "far", "medium", "near", "neighbor", and "close".

The range and size of grid are as follows.

Table II–3–3 Range and Size of Grid for Topographic Corrections

Kinds of Correction	Range radius (km)	Grid Interval X (m) (min)	Grid Interval Y (m) (min)	Topographic Map Used
Far	16.00 – 64.00	7,108 (4′)	7,376 (4′)	1/200,000
Middle	4.00 – 16.00	1,777 (1′)	1,844 (1′)	1/ 50,000
Near	1.00 – 4.00	444.3 (0.25′)	461.0 (0.25′)	1/ 50,000
Neighbour	0.02 – 1.00			1/ 25,000
Close	0.00 – 0.02			sketch

The range of correction listed above means the radius of a circular plate with the gravity station as its center and without overlapping.

(a) Terrain correction of far, medium and near

For the correction of far, medium and near, altitude informations are based on the grid of latitude and longitude of a cartesian co-ordinate and the altitudes are read by a circular plate shown in Fig. II–3–4.

Table II–3–2 Gravity Standard Values

	13159C Tokyo	Muntinglupa	Buguias 900	BM 6642
Latitude	N 35° 38.6′	N 14° 22.5′	N 16° 43.4′	N 36° 50.6′
Longitude	E 139° 41.3′	E 121° 0.9′	E 120° 49.5′	E 139° 43.9′
Date of Observation	1981. 1. 16	1981. 1. 23	1981. 1. 30	1981. 5. 19
Time of Observation	14 h 39 m	18 h 6 m	8 h 2 m	9 h 12 m
Reading Value	3349.406	2020.060	1878.652	3421.386
Instrument Height (m)	0.21	0.27	0.23	0.26
Milligal Value	3562.851	2147.976	1997.565	3639.484
Earth Tide Correction (mgal)	− .073	− .035	− .0007	.072
Instrument Correction (mgal)	0.065	0.083	0.071	0.080
Corrected Value (mgal)	3562.843	2148.024	1997.629	3639.636
Drift Correction (mgal)	0.000	− 0.019	− 0.037	− 0.233
Corrected Value (mgal)	3562.843	2148.005	1997.692	3639.403
Gravity Difference (mgal)	0.000	(976218.464) 1414.838	(976218.465)	76.560
Gravity Value (mgal)	979763.190	978366.470	978216.057	979839.750

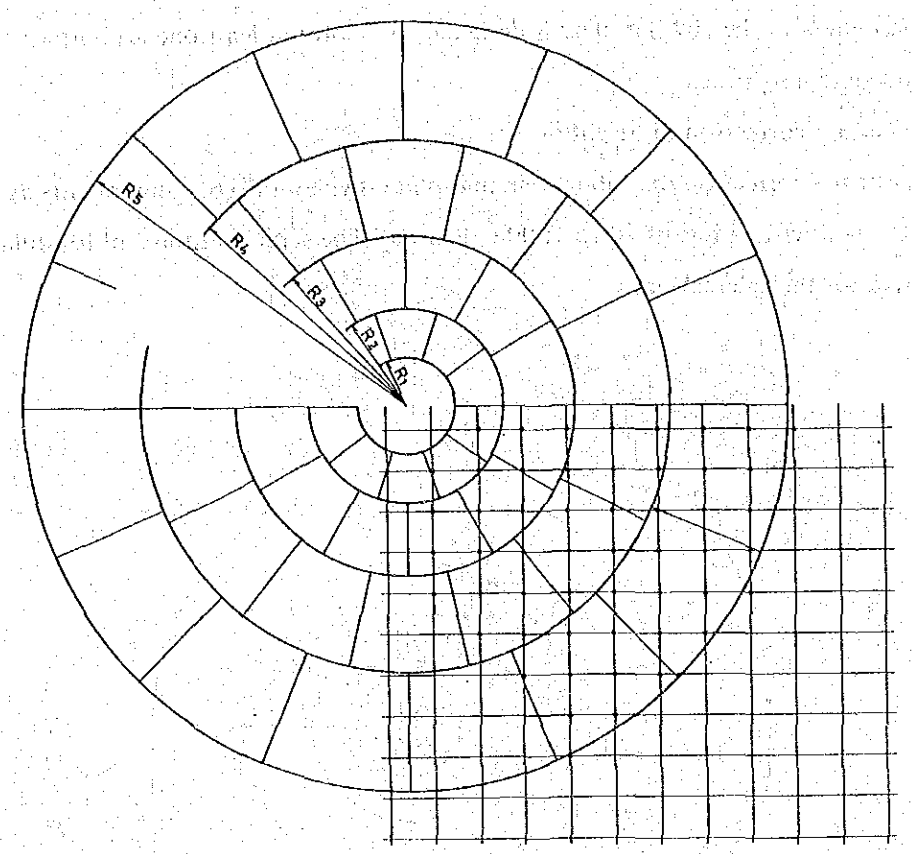

Fig. II–3–4 Disc Used for Topographic Correction (Far, Middle and Near)

Average of all altitudes in each component is used for the correction and total computed terrain correction by a formula shown below is called far, medium or near depending upon the size of the radius.

$$\delta go' = \frac{2\pi}{n} G\rho \left(R_1 - R_2 - \sqrt{R_1^2 + (H - H')^2} + \sqrt{R_2^2 + (H - H')^2} \right)$$

where,

$\delta go'$	:	Terrain correction
n	:	Number of component
G	:	Gravitaional constant
ρ	:	Correction density
R_1	:	Shorter radius of a component
R_2	:	Longer radius of component
$H - H'$	:	Difference of altitude between station and average height of a component

A component in the circular plate is designed to involve at least one grid intersection of latitude and longitude.

(b) Terrain correction of neighbor

For the correction of neibor a circular plate divided into 66 components as shown in Fig. II–3–5 with radius of 20 to 1000 m is used. The same method and formula are adopted for the calculation.

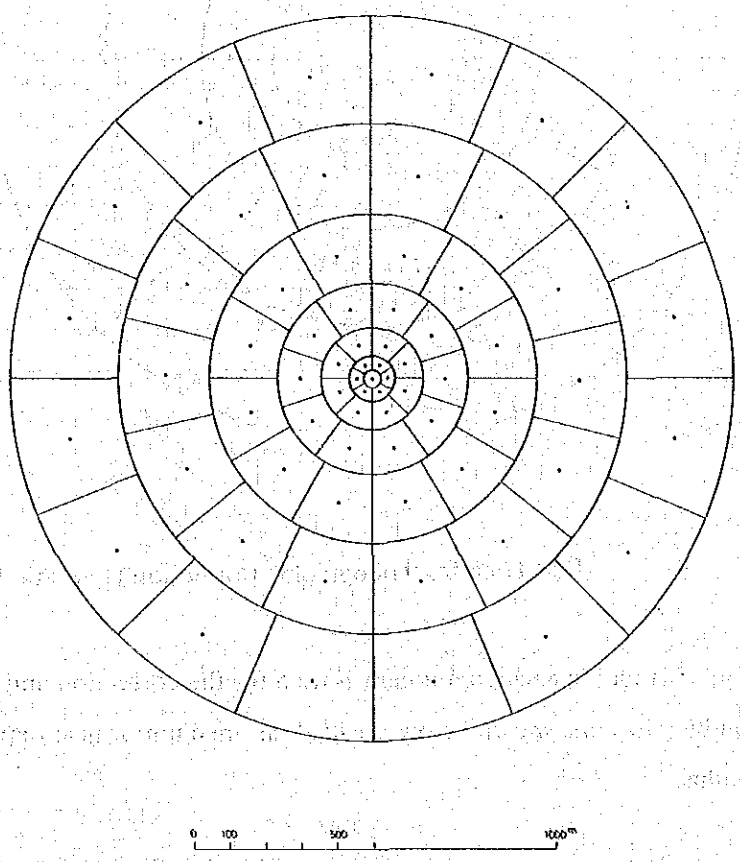

Fig. II–3–5 Disc Used for Topographic Correction (Neibour)

(c) Terrain correction of close

The nearest topography within 20 m from the gravimeter is sketched and a two-dimensional topographic section is simply modified as mentioned below. The correction due to the close cliff, slope and channel are calculated as,

$$\delta g_0' = G\rho \int_D^R \int_{-\sqrt{R^2-X^2}}^{\sqrt{R^2-X^2}} \int_0^{H+(X-D)\tan\beta} \frac{Z\, dXdYdZ}{(X^2+Y^2+Z^2)^{3/2}}$$

$$= 2G\rho \int_{D}^{R} \int_{-\sqrt{R^2-X^2}}^{\sqrt{R^2-X^2}} \left(\frac{1}{\sqrt{X^2+Y^2}} - \frac{1}{\sqrt{X^2+Y^2+(H-D\tan\beta)^2}} \right) dXdY$$

$$= 2G\rho \int_{D}^{R} \left(\log \left| \frac{R-\sqrt{R^2-X^2}}{R+\sqrt{R^2-X^2}} \right| - \log \left| \frac{\sqrt{R^2+(H-D\tan\beta+X\tan\beta)^2} - \sqrt{R^2-X^2}}{\sqrt{R^2+(H-D\tan\beta+X\tan\beta)^2} + \sqrt{R^2-X^2}} \right| \right) dX$$

This integration can not expressed by a primary function, then a digital integration by means of Simpson 1/3 law is used.

When the terrain is rugged, the topography should be divided into many blocks as shown below and the summation of each calculated values becomes the total correction of close.

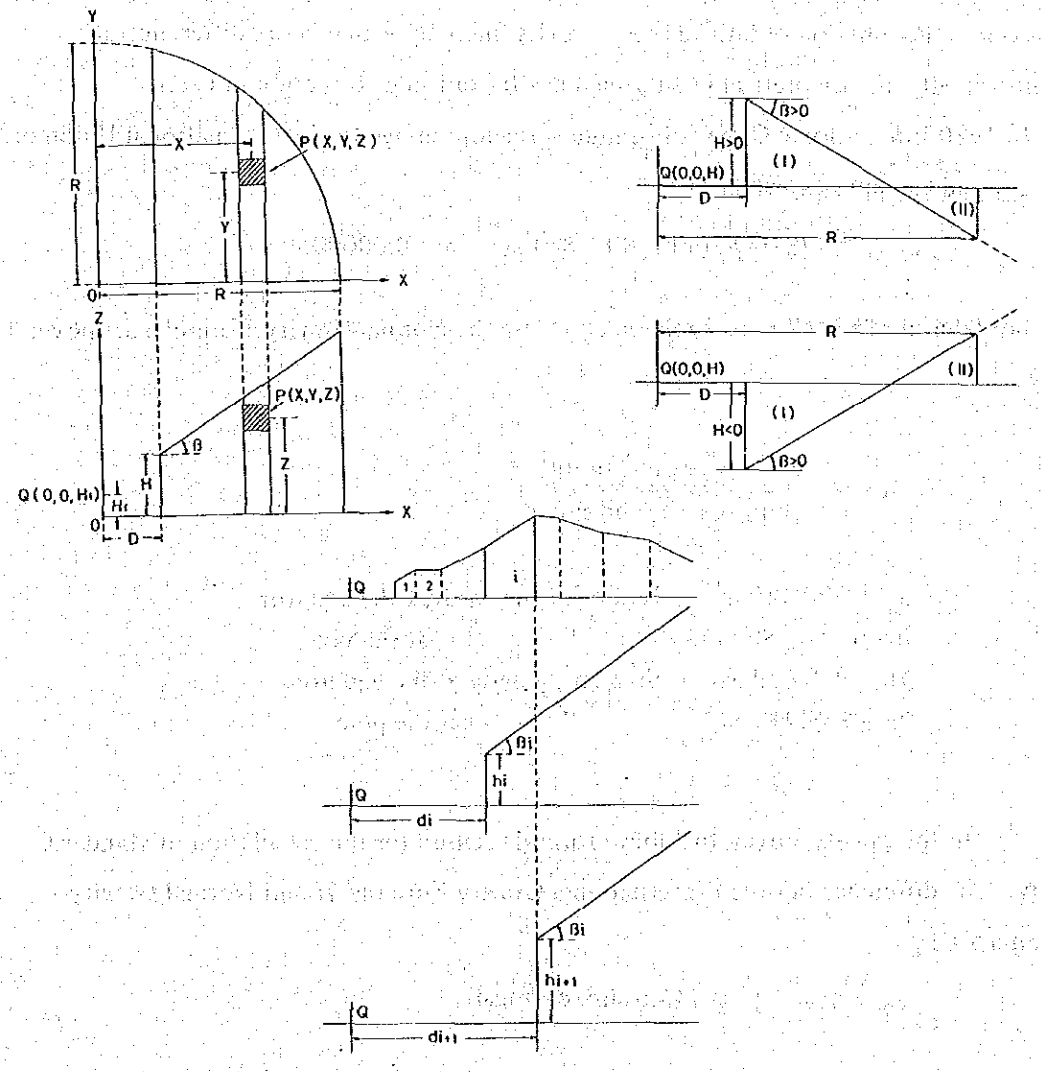

(3) Bouguer correction

Bouguer correction is one of the height correction caused by the attraction of the rock mass between the station and the sea level or the absent mass between them. Bouguer correction is given as follows;

$$\delta go'' = -2\pi G\rho Hm = -0.0419\rho\ Hm$$

Hm : Altitude of the station in meter

ρ : Specific gravity (density) of the intervening rock

(4) Latitude correction

The attraction of gravity on earth decreases towards the equator and increase towards poles because of the centrifugal force resulting from earth's rotation and of the earth's radius due to polar flattening.

As it is the function of latitude ϕ , gravity anomaly which is the difference of absolute gravity and theoretical gravity includes the latitude correction in itself.

In 1930 International Gravity Formula was adopted by IUGG (International Union of Geodesy and Geophysics) which is,

$$\gamma_{1930} = 978.0490\ (1+0.0052884\ \sin^2\ \phi - 0.0000059\ \sin^2\ 2\phi\ )$$

but later in 1967 IUGG recommended to use the Normal Gravity Formula, as shown below,

$$\gamma_{1967} = \frac{a\gamma_E\ \cos^2\ \phi\ + b\gamma_p\ \sin^2\ \phi}{\sqrt{a^2\ \cos^2\ \phi + b^2\ \sin^2\ \phi}}$$

a = 6,378,140 m : Radius of the earth at the equator

b = 6,356,180 m : " at the pole

γ_E = 978.032 gal : Standard gravity at the equator

γ_p = 983.218 gal : " at the pole

In this gravity survey the above formula is used for the calculation of standard gravity. The difference between International Gravity Formula γ_I and Normal Gravity Formula γ_N is,

$$\gamma_N - \gamma_I = -17.2 + 13.6\ \sin^2\ \phi\ \text{(mgal)}$$

(5) Bouguer anomaly

The difference between the corrected gravity value resulting from the above mentioned corrections and the standard gravity, is called Bouguer anomaly,

$$\Delta go'' = g + \delta go + \delta go' + \delta go'' - \gamma_1$$

$\Delta go''$: Bouguer anomaly value

The Bouguer anomaly depends on rock densities. Six density maps have been made (densities of 2.0, 2.40, 2.50, 2.60, 2.67 and 2.70) for both density and terrain.

3–4 Method of Analysis

Results of this investigation are qualitatively and quantitatively interpreted using filtered gravity detected by Fourier analysis. Bouguer anomaly is divided into several "band" by filtering and the residual gravity for each band are used for stractural analysis corresponding with each wave length.

3–4–1 Density Assumption

Although only one assumption is necessary in the analysis of data derived from the gravity survey, it is difficult to interpret geological structure by using only one density data. Assumption of the proper density has been made in several ways as mentioned below and by their combination.

(a) *Density of Rock Samples*

In this survey, 136 rock samples were collected on the ground surface by the geological team and measured their densities by Philippino staff. The average densities and the deviation are shown on Table II–3–4. Quaternary rocks are mainly pumice tuff which is so fragile that it is hard to measure the density. But the density is considered to be around 2.2. The average densities of the upper Tertiary is 2.39, the lower Tertiary 2.57 and intrusive rocks 2.60. Consequently, three layered density model is supposed with the upper density as 2.2, middle as 2.4 and the basement as 2.6 intruded by 2.6 rocks. The total average of all rock samples are 2.56 and the pre-Tertiary is assumed to be 2.8.

Table II–3–4 Average Density of Rock Sample

Period	Formation	Rock (Number of Sample)	Average		Density 2.0 2.2 2.4 2.6 2.8 3.0
Quaternary	Bodo	Pumice Tuff			Unmeasured
Tertiary	Lo–o	Andesite (7)	2.50	2.39	2.32 — 2.72
		Tuff (9)	2.31		2.02 — 2.62
	Buguias	Andesite (24)	2.65	2.57	2.25 — 2.90
		Basalt (5)	2.72		2.39 — 2.98
		Tuff (43)	2.52		1.89 — 2.94
		Mud St., Limestone (3)	2.57		2.39 — 2.65
Intrusive Rock		Andesite (21)	2.62	2.60	2.26 — 2.86
		Diorite (13)	2.67		2.40 — 2.86
		Dacite (3)	2.47		2.40 — 2.61
		Rhyolite (6)	2.40		2.04 — 2.70
		Granite (2)	2.83		2.78 — 2.88

(b) G–H Correlation

Gravity decreases with the altitude of measurement. The rate of decrement is nearly equal to the coefficient of altitude correction, $0.3086-0.0419\rho$. Therefore, when the gravity data are plotted as the altitudes on one axis and latitude corrected gravity on the other axis, the inclination of the linear line fit to the plots represents the average of rock densities in the area. Fig. II–3–1 shows the G–H correlation for this case and the calculated density is 2.56 by least square method.

(c) Determination of Correction Density

The correction density is determined to be 2.6 from both the average density and G–H correlation. Bouguer anomaly maps were drawn for two cases of density $\rho = 2.50$ and $\rho = 2.60$, and better correlation with the geological structure was observed in the case of $\rho = 2.60$, which is used for interpretation.

3–4–2 Residual Gravity

For the purpose of selective dedtection of gravity anomaly of a certain scale, residual

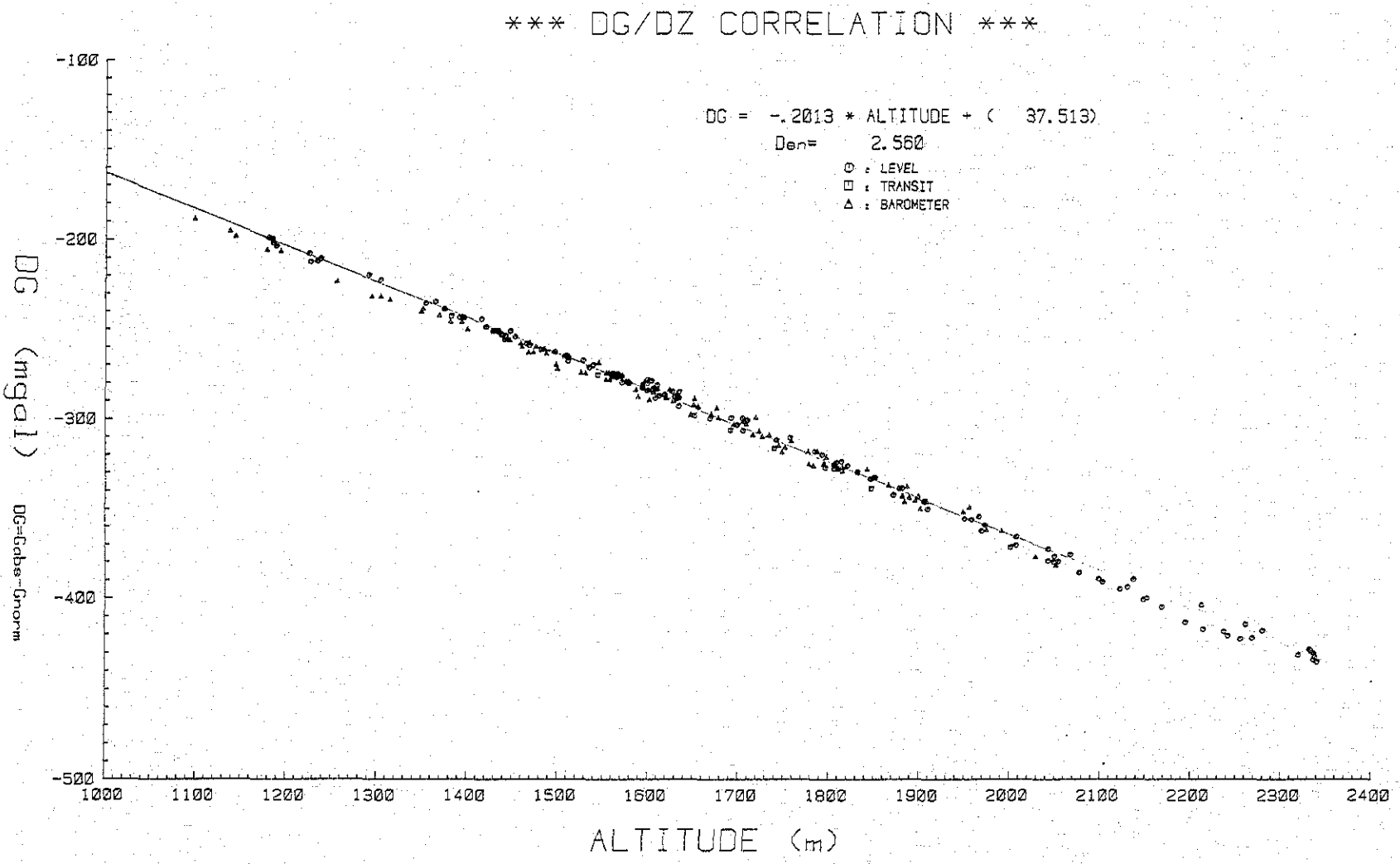

Fig. II–3–6 G–H Correlation Map

gravity is derived from Bouguer anomaly by use of high cut filtering method.

When the gravity potential converted into complex Fourier transform is F (u, v) and number of grid in x and y direction are m and n respectively, this transform is expressed as follows,

$$F(u, v) = \sum_{m} \sum_{n} G(x, y) \cdot \exp(-i(ux+vy)) \Delta x \Delta y$$

$$G(x, y) = \sum_{m} \sum_{n} F(u, v) \cdot \exp(i(ux+vy)) \Delta u \Delta v$$

If the relation between the above equations is expressed as G9(x, y) F9(u, v), high cut filter is obtained as,

$$G(x, y) = F(u, v) \cdot \exp(-\lambda(u^2 + v^2))$$

where, λ is a parameter corresponding with a wave length of high cut filter, and in this processing four kinds of residual gravity are obtained with the parameter of λ = 0.25, 1.8, 9.5 such as $\lambda_{0.25} = (G - G_{0.25})$, $\lambda_{0.25 \sim 1.8} = (G_{0.25} - G_{1.8})$, $\lambda_{1.8 \sim 9.5} = (G_{1.8} - G_{9.5})$ and $\lambda_{9.5} = (G_{9.5})$ and the latter three are indicated in Fig. II–3–10, Fig. II–3–11 and Fig. II –3–12.

3–4–3 Two-Dimentional Section Analysis

Geological structure causing the gravitational anomaly is assumed to be as follows;

(1) Polygonal structures with different density

(2) Stratified structure of which density increase with the depth

(3) Two layered structure with sediments of constant density and the basement

Judging from the geological structure and its residual gravity, either of the structures and their combinations are generally applied.

In this case as an advanced method of interpretation, Fourier transform and Talwani's method are adopted.

(1) Fourier Transform

When F(w) is a Fourier transformed Bouguer gravity g(x) and density does not change down to the depth of D, gravity at the depth of D is expressed as exp (Dw) · F (w) by the theory of downward-continuation. This gravitational anomaly is equivalent with that of

the condensed density, $2\pi G\rho^*(w)$ at the depth D, where $\rho^*(w)$ is the condensed density at the depth D. In case of two-layered structure with the density difference of $\Delta\rho$ the relation becomes $\rho^*(w) = \Delta\rho H(w)$, where H(w) is the change of basement depth in the frequency domain. Then, a basement depth h(x) is derived from the reverse Fourier transform of H(w).

(2) Talwani's Method

In two-dimentional section analysis, Bouguer values calculated from an assumed density structure are compared with observed Bouguer values. The density structure is modified until the calculated Bouguer values fit well with the observed values by trial and error. Calculation of Bouguer values is performed by an electronic computer using Talwani's fomula, taking the lateral effect of anomaly into consideration.

$$\Delta g = 2G\Delta\rho \sum Z_i$$

$$Z_i = \frac{(x_{i+1} - X_i)\left\{Z_i(X - X_{i+1}) - Z_{i+1}(x - x_i)\right\}}{(x_{i+1} - x_i)^2 + (z_{i+1} - Z_i)^2}$$

$$\times \quad \tan^{-1}\left\{\frac{Z_i}{x_i - x} - \tan^{-1}\frac{Z_{i+1}}{x_{i+1} - x} + \frac{1}{2}\frac{Z_{i+1} - Z_i}{x_{i+1} - x_i}\log\frac{(x_{i+1} - x)^2 + Z_{i+1}^2}{(x_i - x)^2 + Z_i^2}\right\}$$

When an edge of a polygon is rectangle ($x_i = x_{i+1}$)

$$Z_i = \frac{x_i - x}{2}\log\frac{(x_i - x)^2 + Z_{i+1}^2}{(x_i - x)^2 + Z_i^2}$$

and a surface of a polygon is horizontal ($z_i = z_{i+1}$),

$$Z_i = -Z_i\left(\tan^{-1}\frac{Z_i}{x_i - x} - \tan^{-1}\frac{Z_i}{x_{i+1} - x}\right)$$

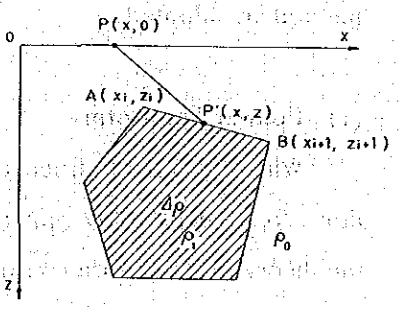

3–5 Interpretation

Data of this gravity survey, such as Bouguer anomaly and the residual gravity maps are qualitatively and quantitatively treated in the following manner.

3–5–1 Bouguer Anomaly Map

Among the assumed density of 2.0 to 2.7 four kinds of densities are used to make Bouguer anomaly maps. Topography of this area is so steep that a pattern of the contour map considerably changes by a slight change of density of 0.1. On Fig. II–3–7, II–3–8 and II–3–9 Bouguer anomalies are shown with the density of 2.5, 2.6 and 2.7 respectively. Among them, assumed density 2.60 (Fig. II–3–8) is selected as it reflects the geological structure better than others with less terrain effects.

Bouguer anomaly values varying from 39 mgal to 53 mgal, shows that the area investigated is mainly controlled by N–S trending structure judging from the tendency of the contour flow. If the high gravity anomalies are defined as Bouguer anomaly greater than 46 mgal and low gravity less than 42 mgal comparatively, high gravity anomalies generally surround the low gravity anomalies, just as seen in the western area around Sinepsip, south-eastern area around Lutab to Kabayan and north-eastern area from Tangawan. Low gravity anomalies are developed in the central part and dominant N–S trend low gravity zone are seen along Pulibo Ridge to Harshima road. Furthermore, from south of Buguias Central low gravity zone streaching eastwards to Ifgao province has been detected.

Among those anomalies, prominent N–S low gravity zone suggests east dipping fault along west Pulibo Ridge forming the western margin of big scale graben structure.

The other east dipping fault, cutting high gravity anomally along Toking creek runs from Dalimona to Bodo showing an interesting structure for geothermal reservoir. Low gravity anomaly from this fault seems to extend towards Ifgao side and extension of gravity survey in the future would enhance the image of the geothermal system.

3–5–2 Residual Gravity

Residual gravity maps are shown in Fig. II–3–10, II–3–11 and II–3–12. Through the filtering of Fourier transform, there are no lacking of data on the frame of the surveyed area. Parameter λ which dicides the wave length of filters are 0.25, 1.8 and 9.5 judging from the spectrum analysis. ($\lambda = 1$ corresponds 2 km). A filter with $\lambda = 0.25$ is a low cut filter

emphasizing the noise structure, which does not indicate any meaning. A map shown in Fig. II–3–10 is a residual map with λ = 0.25 – 1.8 which would indicate the structure of about 1.5 km. The map suggests synclynal structure west of Agno river, the fault running from south of Abatan to Dalimona and Bodo in NW–SE trend, another fault south east of Buguias running in NE–SW trend and distribution of intrusive rocks between Dalimona and Buguias. Fig. II–3–11 is a residual map with λ = 1.8–9.5 which would indicate the structure of about 3 to 4 km. This map emphasizes E–W trend structure south of Loo, N–S trend structure seen in the western, notheastern and southeastern side of the area surveyed and also N–S trend synclynal structure in the west of Agno river. The biggest structure, gravitational basement is seen in high cut filter map of λ = 9.5 shown in Fig. II–3–12. A semi-basin structure plunging towards the east, with a diameter of 5 ~ 7 km and its center around Buguias to Tangawan, is believed to exist at depth and maybe indicative of a structure for a geothermal reservoir. The anomaly tends to extend towards the boundary of Ifgao province.

3–5–3 Two-Dimentional Section Analysis

In this survey area, geological structure with N–S trend is dominant so that Bouguer anomaly map is characterized by N–S contours. An E–W section from Sinepsip to Bodoan is selected as two dimentional section analysis. Assuming the densities of the models from the results of density measurement, the first layer would be Quarternary volcanics (ρ_1 = 2.2), the second layer be upper Tertiary igneous rocks ρ_2 = 2.4 and the third layer be lower Tertiary igneous and sedimentary rocks and/or intrusive rocks ρ_3 = 2.6. On this section the first layer is almost lacking and no outcrops of basement rocks are found, so that two dimentional analysis must be done without control-point to decide the depth of the boundary. Then, the assumed densities for each layer are decided as 2.5 ± 0.1, 2.6 ± 0.05 and 2.7 ± 0.05 to calculate the relative depth of the boundary. The block movement of the basement is interpreted from Regional and Residual λ = 1.8 ~ 9.5 and the boundary of the first and the second layer is from regional λ = 0.25 ~ 1.8 and Bouguer. The analyzed section are shown in Fig. II–3–13. A deep penetrating fault is assumed to run in the east of Sinepsip showing the west margin of the big scale graben structure. Many block movement are seen in the shallower zone and an east dipping fault cutting around Bodoan looks promissing structure which could control the shallower geothermal fluid. Most of the analyzed structures coincide well with the geological structure seen on the ground but some

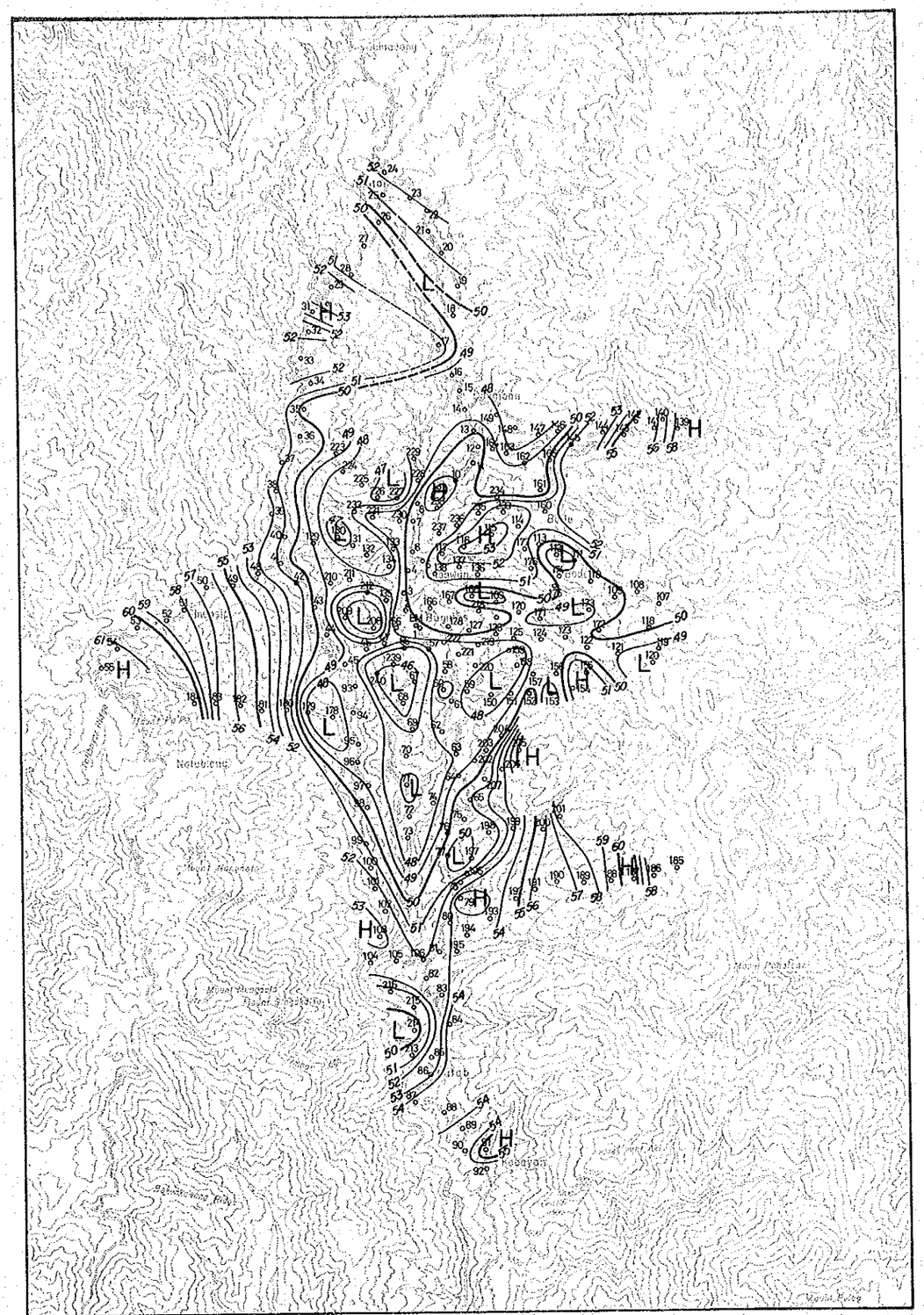

Bugulos Geothermal Development Survey
the Republic of the Philippines

BOUGUER ANOMALY MAP
(ρ = 2.5)

0 1000 6000 km

Jan ~ Feb, 1981

Fig. II-3-7

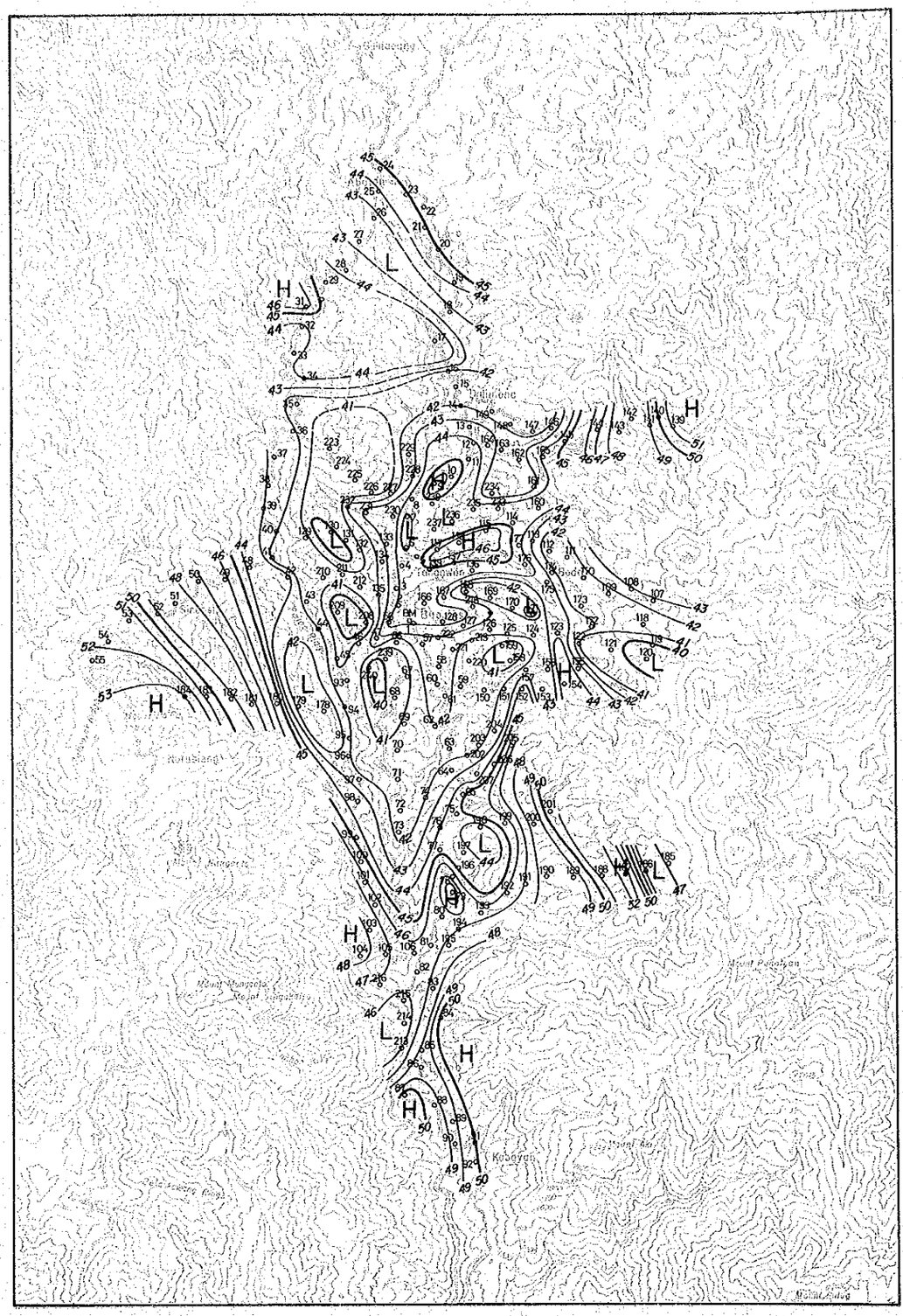

Buguias Geothermal Development Survey
the Republic of the Philippines

BOUGUER ANOMALY MAP
(ρ = 2.6)

0 1000 km 6000

Jan~Feb, 1981. Fig. II-3-8

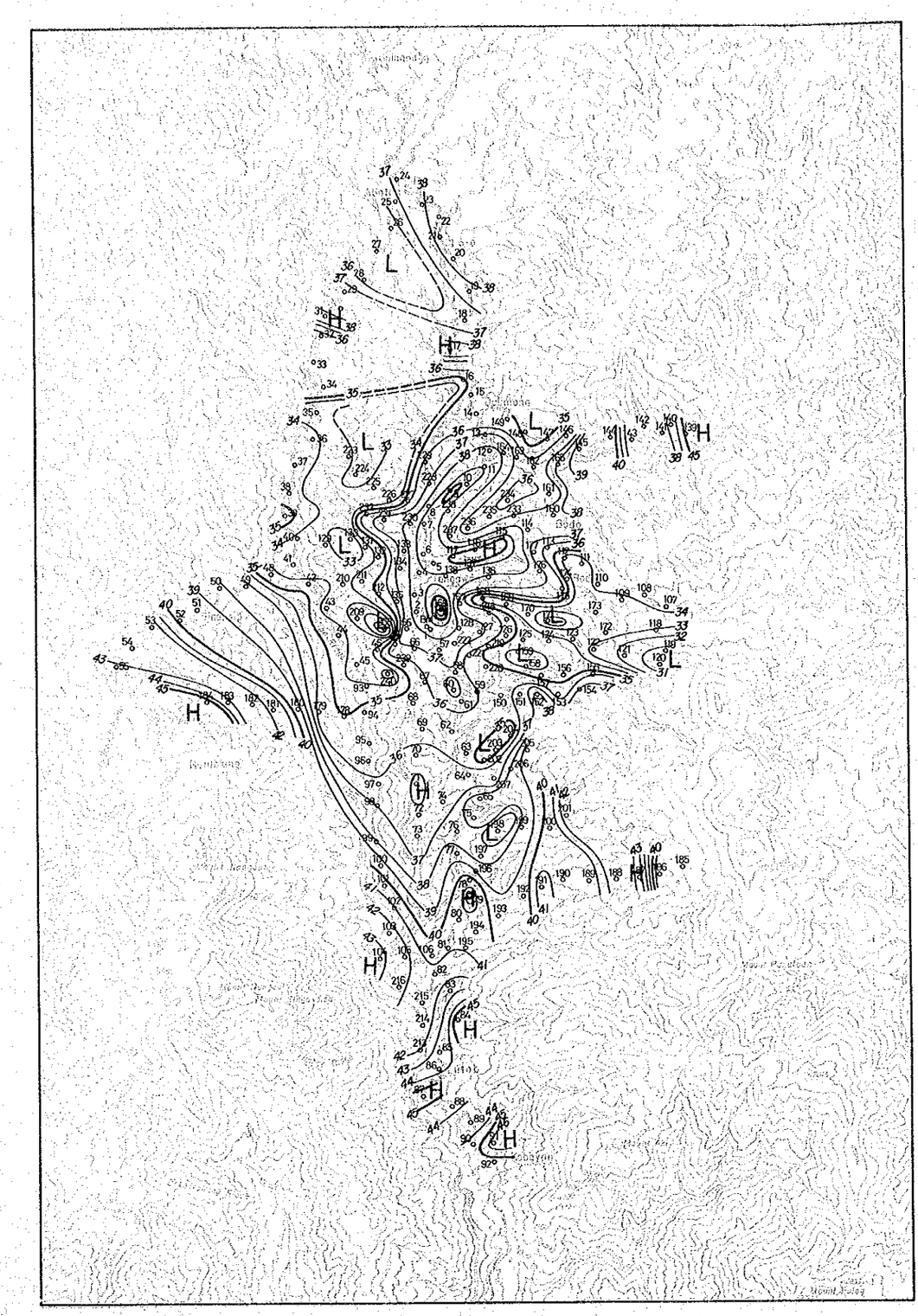

Buguias Geothermal Development Survey

the Republic of the Philippines

BOUGUER ANOMALY MAP

(ρ = 2.7)

0 1000 6000 km

Jan~Feb, 1981

Fig. II-3-9

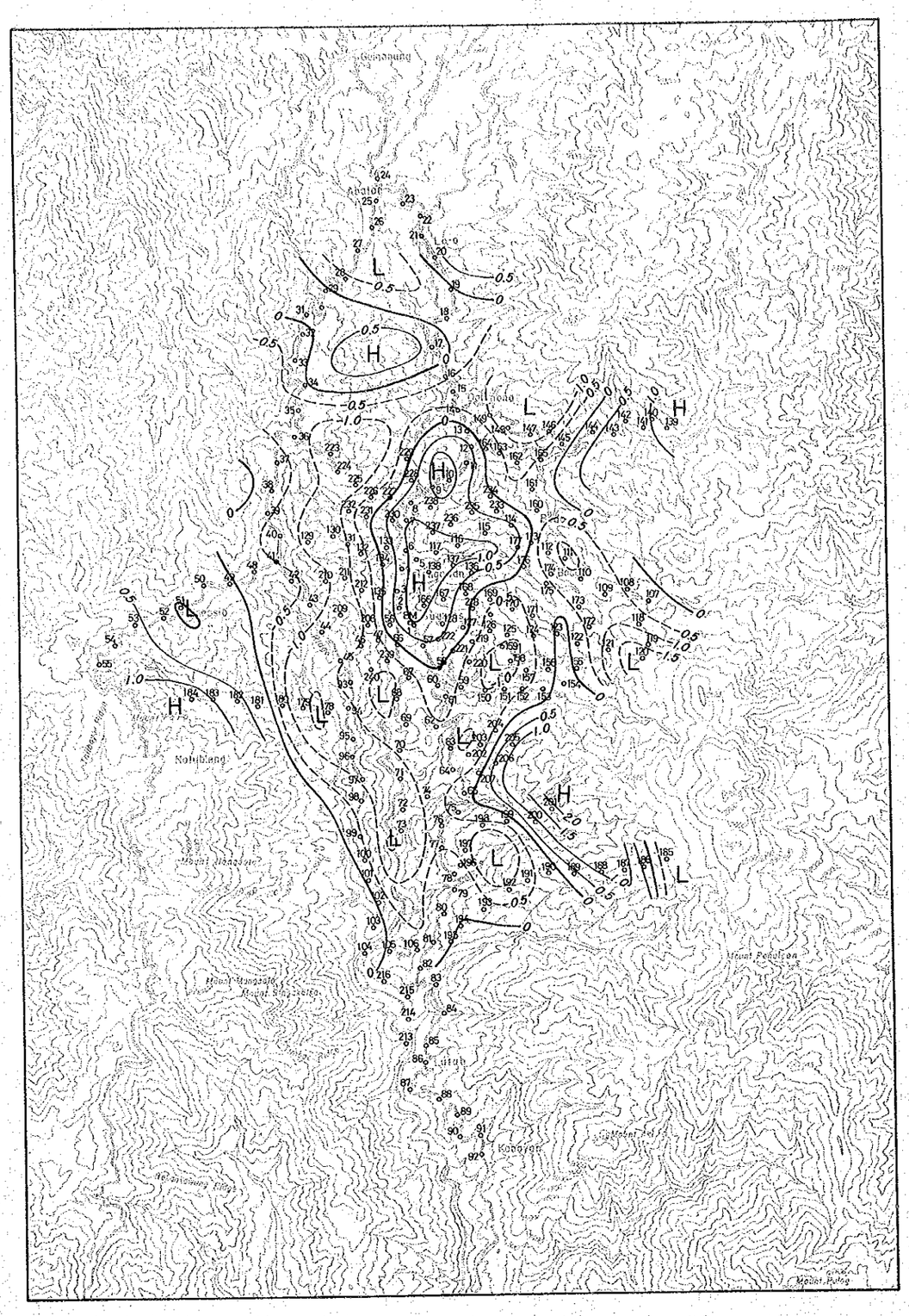

Buguios Geothermal Development Survey

the Republic of the Philippines

RESIDUAL GRAVITY MAP

(λ = 0.25~1.8)

0 1000 6000 km

Jan~Feb, 1981

Fig. II-3-10

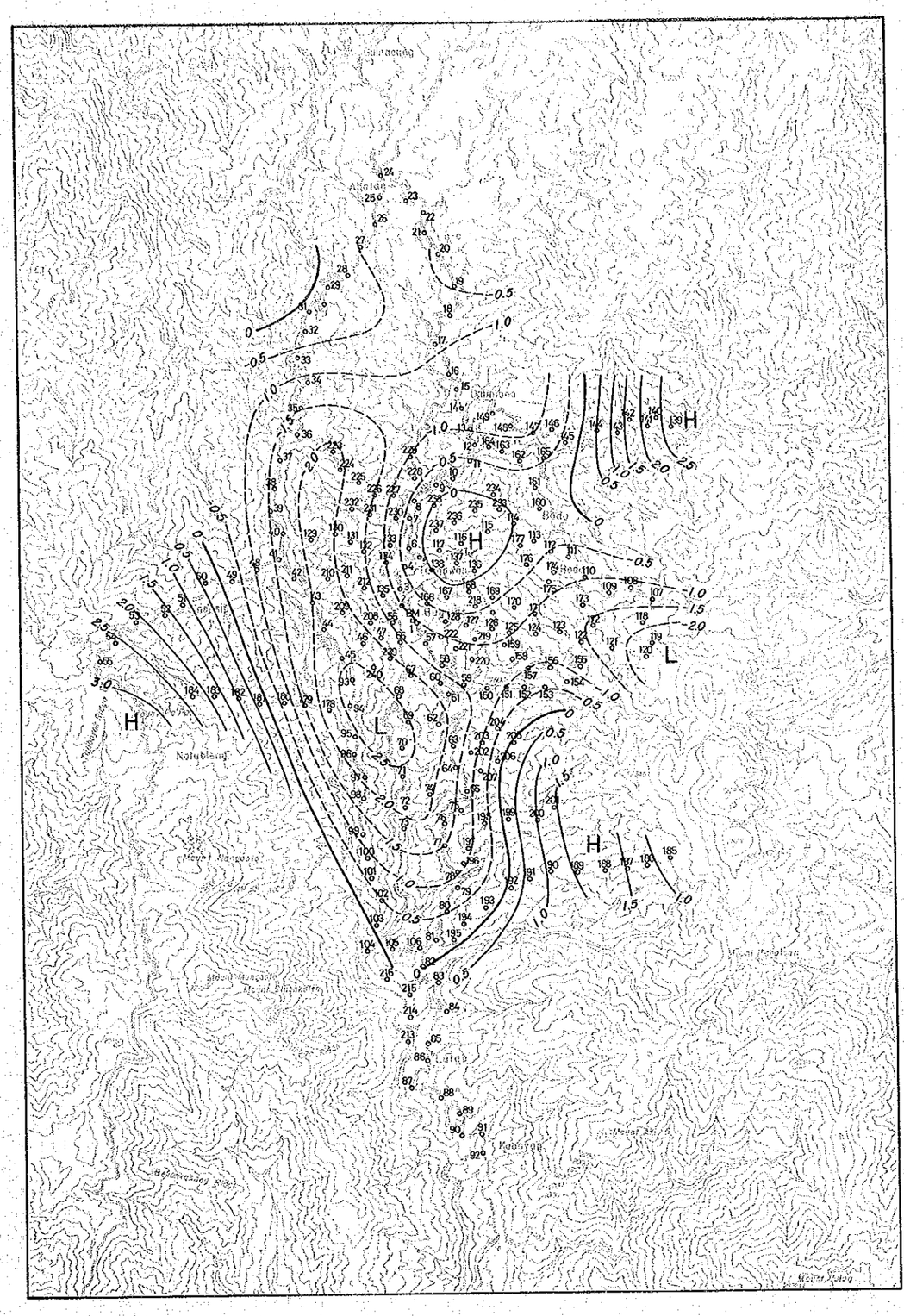

Buguias Geothermal Development Survey

the Republic of the Philippines

RESIDUAL GRAVITY MAP

(λ = 1.8 ~ 9.5)

0 1000 6000 km

Jan ~ Feb, 1981

Fig. II-3-11